Published for SISSA by Springer

Received: *June 24, 2020*
Accepted: *August 18, 2020*
Published: *September 22, 2020*

N-jettiness beam functions at N^{3}LO

Markus A. Ebert,[a] **Bernhard Mistlberger**[b] **and Gherardo Vita**[a]

[a] *Center for Theoretical Physics, Massachusetts Institute of Technology, Cambridge, Massachusetts 02139, U.S.A.*
[b] *SLAC National Accelerator Laboratory, Stanford University, Stanford, CA 94039, U.S.A.*

E-mail: ebert@mit.edu, bernhard.mistlberger@gmail.com, vita@mit.edu

Abstract: We present the first complete calculation for the quark and gluon N-jettiness ($\mathcal{T}_N$) beam functions at next-to-next-to-next-to-leading order (N^{3}LO) in perturbative QCD. Our calculation is based on an expansion of the differential Higgs boson and Drell-Yan production cross sections about their collinear limit. This method allows us to employ cutting edge techniques for the computation of cross sections to extract the universal building blocks in question. The class of functions appearing in the matching coefficents for all channels includes iterated integrals with non-rational kernels, thus going beyond the one of harmonic polylogarithms. Our results are a key step in extending the $\mathcal{T}_N$ subtraction methods to N^{3}LO, and to resum $\mathcal{T}_N$ distributions at N^{3}LL$'$ accuracy both for quark as well as for gluon initiated processes.

Keywords: Perturbative QCD, Resummation

ArXiv ePrint: 2006.03056

https://doi.org/10.1007/JHEP09(2020)143

JHEP09(2020)143

Contents

1 Introduction

Experimental measurements at the LHC have provided remarkably precise measurements for a multitude of observables, most notably weak gauge boson production, an important benchmark for the Standard Model which has been measured at percent level accuracy [1–4]. Strong constraints on physics beyond the Standard Model are also provided by precision measurements of Higgs boson production and diboson processes [5–9]. To make full use of these results, it is crucial to confront them with equally-precise theory predictions, which in particular requires to include higher-order corrections in QCD.

So far, only inclusive Drell-Yan and Higgs production have been calculated at next-to-next-to-next-to-leading order ($\mathrm{N^3LO}$) in QCD [10–17], while significant progress is being made to reach the same precision for differential distributions [18, 19]. A key challenge for such calculations is the cancellation of infrared divergences between real and virtual corrections, and hence a necessary prerequisite is a profound understanding of the infrared singular structure at three loops.

N-jettiness ($\mathcal{T}_N$) is an infrared-sensitive N-jet resolution observable and thus provides a way to study the singular structure of QCD [20, 21]. Its simplest manifestation $\mathcal{T}_0$, also referred to as beam thrust, is defined as

$$\mathcal{T}_0 = \sum_i \min\left\{\frac{2q_a \cdot k_i}{Q_a}, \frac{2q_b \cdot k_i}{Q_b}\right\}, \tag{1.1}$$

where the sum runs over all momenta k_i in the hadronic final state, $q_{a,b}$ are the momenta of the incoming partons projected onto the Born kinematics, and the measures $Q_{a,b}$ distinguish different definitions of $\mathcal{T}_0$ [22, 23]. A key feature of $\mathcal{T}_N$ is that its singular structure as

JHEP09(2020)143

$\mathcal{T}_N \to 0$ is fully captured by a factorization theorem, as shown in refs. [20, 21] using soft-collinear effective theory (SCET) [24–28]. In the simplest case, namely the production of a color-singlet final state h, the appropriate factorization theorem reads

$$\frac{\mathrm{d}\sigma}{\mathrm{d}Q^2\mathrm{d}Y\,\mathrm{d}\mathcal{T}_0} = \sigma_0 \sum_{a,b} H_{ab}(Q^2,\mu) \int \mathrm{d}t_a\,\mathrm{d}t_b\, B_a(t_a,x_a,\mu)\, B_b(t_b,x_b,\mu) \times S_c\left(\mathcal{T}_0 - \frac{t_a}{Q_a} - \frac{t_b}{Q_b},\mu\right)\left[1+\mathcal{O}\left(\frac{\mathcal{T}_0}{Q}\right)\right]. \tag{1.2}$$

Here, Q^2 and Y are the invariant mass and rapidity of h, respectively, and we normalize by the Born partonic cross section σ_0. In eq. (1.2), the full process dependence is given in terms of the hard function H_{ab}, which encodes virtual corrections to the underlying hard process $ab \to h$. The beam functions $B_{a,b}$ encode radiation collinear to the incoming partons. The soft function S_c encodes soft radiation and only depends on the color channel $c \in \{gg, q\bar{q}\}$, but is independent of quark flavors. Both beam and soft functions are universal and process independent. Since they are defined as gauge-invariant matrix elements in SCET, calculating them at higher orders also provides a well-defined means of separately studying the collinear and soft limits of QCD themselves. The beam functions $B_{a,b}$ not only appear in the factorization theorem for all $\mathcal{T}_N$, but also arise in the factorization theorem for the generalized threshold inclusive color-singlet production in hadronic collisions [29], and are thus of particular interest on their own.

Since eq. (1.2) fully captures the singular limit of QCD, it can be employed as a subtraction scheme for higher-order calculations [30, 31], in analogy to the q_T subtraction method based on a similar factorization for the transverse-momentum distribution [32]. For both methods, extensions to N^{3}LO have been recently proposed [18, 33]. The $\mathcal{O}(\mathcal{T}_0/Q)$ corrections to eq. (1.2) have also been studied in the context of $\mathcal{T}_N$ subtractions [34–39].[1] These calculations are also interesting on their own as they provide insights into the infrared structure of QCD beyond leading power. $\mathcal{T}_0$ subtractions are also the basis of combining NNLO calculations with a parton shower in `GENEVA` [41, 42].

Currently, the quark and gluon $\mathcal{T}_N$ beam functions are known at NNLO [43–46], and significant progress has been made towards the calculation at N^{3}LO for the quark case [47–49]. The soft functions required for $\mathcal{T}_{0,1,2}$ are known at NNLO [50–58]. The factorization for $\mathcal{T}_{N\geq 1}$ also requires the so-called jet function, which is also known at N^{3}LO [59–65]. In this paper, we calculate the $\mathcal{T}_N$ beam functions for all partonic channels at N^{3}LO, thereby providing a critical ingredient to extending $\mathcal{T}_N$ subtraction to three loops both for quark as well as for gluon initiated processes.

Our computation is based on a method of expanding cross sections around the kinematic limit in which all final state radiation becomes collinear to one of the scattering hadrons [66]. This method allows one to efficiently connect technology for the computation of scattering cross sections to universal building blocks of perturbative QFT. In particular, we perform a collinear expansion of the Drell-Yan and gluon fusion Higgs boson

[1] For measurements with fiducial cuts applied to h, eq. (1.2) also receives enhanced $\mathcal{O}(\sqrt{\mathcal{T}_0/Q})$ corrections [40].

JHEP09(2020)143

production cross section at N^{3}LO. Subsequently, we employ the framework of reverse unitarity [67–71], integration-by-part (IBP) identities [72, 73] and the method of differential equations [74–78] to obtain the collinear limit of the cross sections differential in the rapidity and transverse momentum of the colorless final states. Using the connection of this limit to the desired beam functions we extract the desired perturbative matching kernels as discussed in ref. [66].

This paper is structured as follows. In section 2, we discuss our setup for calculating the beam functions based on the collinear expansion of ref. [66]. In section 3, we briefly present our results, before concluding in section 4. Our results are also provided in the form of supplementary material with this submission.

2 Beam functions from the collinear limit of cross sections

Since the $\mathcal{T}_N$ beam function is independent of N, we calculate it from the simplest case $\mathcal{T}_0$ by considering the production of a colorless hard probe h and an additional hadronic state X in a proton-proton collision,

$$P(P_1) + P(P_2) \quad \to \quad h(-p_h) + X(-k)\,, \tag{2.1}$$

where the incoming protons are aligned along the directions

$$n^\mu = (1,0,0,1)\,, \qquad \bar{n}^\mu = (1,0,0,-1) \tag{2.2}$$

and carry the momenta P_1 and P_2 with the center of mass energy $S = (P_1 + P_2)^2$. The hard probe h carries the momentum p_h, and the total momentum of the hadronic final state is denoted as k. We parameterize these momenta in terms of

$$Q^2 = p_h^2\,, \quad Y = \frac{1}{2}\ln\frac{\bar{n}\cdot p_h}{n\cdot p_h}\,, \quad w_1 = -\frac{\bar{n}\cdot k}{\bar{n}\cdot p_1}\,, \quad w_2 = -\frac{n\cdot k}{n\cdot p_2}\,, \quad x = \frac{k^2}{(\bar{n}\cdot k)(n\cdot k)}\,, \tag{2.3}$$

where Q^2 and Y are the invariant mass and rapidity of the hard probe h, respectively.

Eq. (2.1) receives contributions from the partonic process

$$i(p_1) + j(p_2) \quad \to \quad h(-p_h) + X_n(-p_3,\ldots,-p_{n+2})\,, \tag{2.4}$$

where i and j are the flavors of the incoming partons which carry the momenta p_1 and p_2, and X_n is a hadronic final state consisting of n partons with the momenta $\{-p_3,\ldots,-p_{n+2}\}$, and $n = 0$ at tree level. The cross section for the partonic process in eq. (2.4), differential in the variables defined in eq. (2.3), is then defined as

$$\frac{\mathrm{d}\eta_{ij}}{\mathrm{d}Q^2\mathrm{d}w_1\mathrm{d}w_2\mathrm{d}x} = \frac{1}{\sigma_0}\frac{\mathcal{N}_{ij}}{2S}\sum_{X_n}\int\frac{\mathrm{d}\Phi_{h+n}}{\mathrm{d}w_1\mathrm{d}w_2\mathrm{d}x}\,|\mathcal{M}_{ij\to h+X_n}|^2\,. \tag{2.5}$$

Here, we normalize by the partonic Born cross section σ_0, $\mathrm{d}\Phi_{h+n}$ is the phase space measure of the $h + X_n$ state, and $|\mathcal{M}_{ij\to h+X_n}|^2$ is the squared matrix element for the process in eq. (2.4), summed over the colors and helicities of all particles, with $\mathcal{N}_{ij}$ accounting for

JHEP09(2020)143

the color and helicity average of the incoming particles. Explicit expressions for $\mathcal{N}_{ij}$ and $\mathrm{d}\Phi_{h+n}$ can be found in ref. [66].

The partonic cross section in eq. (2.5) is closely related to the beam function we are interested in. For perturbative values of $\mathcal{T}_N$, one can match the beam functions onto the PDFs as [20, 43]

$$B_i(t,z,\mu) = \sum_j \int_z^1 \frac{\mathrm{d}z'}{z'}\, \mathcal{I}_{ij}(t,z',\mu)\, f_j\left(\frac{z'}{z},\mu\right) \times \left[1+\mathcal{O}\left(\frac{\Lambda^2_{\mathrm{QCD}}}{t}\right)\right]. \tag{2.6}$$

Here, $\mathcal{I}_{ij}$ is a perturbative matching kernel, and $t = \mathcal{T}_0 Q_a$, see eq. (1.2). As shown by us in ref. [66], $\mathcal{I}_{ij}$ is precisely given by the strict n-collinear limit of eq. (2.5), where all loop and real momenta are treated as being collinear to n-direction, and we refer to ref. [66] for details on how to calculate this limit:

$$\begin{aligned}\mathcal{I}_{ij}(t,z,\epsilon) = \int_0^1 \mathrm{d}x \int_0^\infty \mathrm{d}w_1 \mathrm{d}w_2\, \delta[z-(1-w_1)]\delta(t-Q^2 w_2) \\ \times \lim_{\text{strict } n-\text{coll.}} \frac{\mathrm{d}\eta_{ij}}{\mathrm{d}Q^2 \mathrm{d}w_1 \mathrm{d}w_2 \mathrm{d}x}.\end{aligned} \tag{2.7}$$

Here, we have regulated both UV and IR divergences by working in $d = 4-2\epsilon$ dimensions. The renormalized matching kernel is then given by [43, 44, 66]

$$\mathcal{I}_{ij}(t,z,\mu) = \sum_k \int \mathrm{d}t'\, Z_B^i(t-t',\epsilon,\mu) \int_z^1 \frac{\mathrm{d}z'}{z'}\, \Gamma_{jk}\left(\frac{z}{z'},\epsilon\right) \hat{Z}_{\alpha_s}(\mu,\epsilon)\, \mathcal{I}_{ik}(t',z',\epsilon)\,. \tag{2.8}$$

Here, $\hat{Z}_{\alpha_s}$ implements the standard UV renormalization by renormalizing the bare coupling constant α_s^b in the $\overline{\mathrm{MS}}$ scheme, and the convolution with the PDF counterterm Γ_{jk} cancels infrared divergences. Explicit expressions for these ingredients are collected in appendix A.3. The remaining poles in ϵ are canceled by the convolution with the beam function counter term Z_B, which in the formulation of the beam function within SCET arises as an additional UV counter term in effective theory.

3 Results

In this section we report on our results for the matching kernels through N^{3}LO. Our computation is based on the collinear expansion of the cross sections for the production of a Higgs boson via gluon fusion and for the production of off-shell photon (Drell-Yan) in hadron collisions. We compute the Higgs boson production cross section in the heavy top quark effective theory where the degrees of freedom of the top quark were integrated out and the Higgs boson couples directly to gluons [79–87].

We begin by computing all required matrix elements with at least one final state parton to obtain N^{3}LO cross sections. All partonic cross sections corresponding to matrix elements with exactly one parton in the final state were obtained in full kinematics for the purpose of refs. [17, 88–90] and are in part based on refs. [91–93]. In order to obtain the strict collinear limit we simply expand the existing results and select the required components.

JHEP09(2020)143

To compute partonic cross sections with more than one final state parton we generate the necessary Feynman diagrams using QGRAF [94] and perform spinor and color algebra in a private code. Subsequently, we perform the strict collinear expansion of this matrix elements as outlined in ref. [66]. We make use of the framework of reverse unitarity [67–71] in order to integrate over loop and phase space momenta. We apply integration-by-part (IBP) identities [72, 73] in order to re-express our expanded cross section in terms of collinear master integrals depending on the variables introduced in eq. (2.3). We then compute the required master integrals using the method of differential equations [74–78]. In order to fix all boundary conditions for the differential equations we expand the collinear master integrals further around the soft limit and integrate over phase space (see ref. [66] for more details). The result of this procedure is then easily matched to the soft integrals that were obtained for the purpose of refs. [10, 15, 95–97].

This yields all required ingredients for the bare partonic cross section expanded in the strict collinear limit of eq. (2.5). This part of the computation is the same as for the results of ref. [98]. Next, we perform the Fourier transform over t and make use of eq. (2.7) to obtain the matching kernel through N^{3}LO in QCD perturbation theory. We will elaborate on the details of the computation of the matching kernels in ref. [99]. Finally, we subtract poles in ϵ as given in eq. (2.8) to obtain the renormalized matching kernel $\mathcal{I}_{ij}(t, z, \mu)$ through N^{3}LO in QCD perturbation theory. This is carried out in Fourier (y) space, where the convolution in t becomes a simple product, and the Fourier-transformed counter term $\tilde{Z}_B$ can be easily predicted from the known renormalization group equation (RGE) of the beam function. We collect the required formulas in appendix A.2. It straightforward to Fourier transform back to t space after the UV renormalization, and we will provide results in both spaces.

We express the perturbative matching kernels in terms of harmonic polylogarithms [100] and Goncharov polylogarithms [101] as well as a set of iterated integrals. We define the iterated integrals recursively via

$$J\big(a_1(z), a_2(z), \ldots, a_n(z)\big) = \int_0^z \mathrm{d}x\, a_1(x)\, J\big(a_2(x), \ldots, a_n(x)\big)\,, \tag{3.1}$$

with the prescription to regularize logarithmic singularities as

$$J\left(\frac{1}{z}\right) = \int_1^z \frac{dx}{x} = \log(z). \tag{3.2}$$

We refer to the arguments of the iterated integrals as letters. The explicit end point of the iterated integration used for our iterated integrals is always the variable $\bar{z} = 1 - z$. In order to express our matching kernels we require the following set of letters (or alphabet):

$$\mathcal{A} = \left\{\frac{1}{z}, \frac{1}{1-z}, \frac{1}{2-z}, \frac{1}{1+z}, \frac{1}{\sqrt{4-z}\sqrt{z}}\right\}. \tag{3.3}$$

It is possible to rationalise the square root in $\mathcal{A}$ by introducing the variable transformation $z \to (y+1)^2/y$ as noted in ref. [49] and to rewrite the iterated integrals in terms of Goncharov polylogarithms using well known techniques, see for example refs. [102–105].

JHEP09(2020)143

Studying the letters of our alphabet and the singularities appearing in our matching kernels we see that they contain logarithmic singularities at the boundaries of the physical interval $z \in [0,1]$. In order to provide a representation of our perturbative matching kernels that is suitable for numeric evaluation we perform a generalised power series expansion around two different points $z = 0$ and $z = 1$ up to 50 terms in the expansion. Both power series are formally convergent within the entire unit interval but converge of course faster if the respective expansion parameter is smaller. We provide both power series for all matching kernels as well as the analytic solution in the supplementary material of this article.

We have calculated the matching kernel in Fourier (y) space, where its renormalization becomes simpler. As it is more commonly used in momentum (t) space, we provide results in both spaces. The corresponding kernels are expanded in powers of α_s/π,

$$\tilde{\mathcal{I}}_{ij}(y,z,\mu) = \sum_{n=0}^{\infty} \left(\frac{\alpha_s}{\pi}\right)^n \tilde{\mathcal{I}}_{ij}^{(n)}(y,z,\mu)\,, \qquad \mathcal{I}_{ij}(t,z,\mu) = \sum_{n=0}^{\infty} \left(\frac{\alpha_s}{\pi}\right)^n \mathcal{I}_{ij}^{(n)}(t,z,\mu)\,. \tag{3.4}$$

The coefficients $\tilde{\mathcal{I}}_{ij}^{(n)}$ and $\mathcal{I}_{ij}^{(n)}$ can be further expanded as

$$\begin{aligned}
\tilde{\mathcal{I}}_{ij}^{(n)}(y,z,\mu) &= \tilde{I}_{ij}^{(n)}(z) + \sum_{m=1}^{2n} \tilde{\mathcal{I}}_{ij}^{(n,m)}(z) L_y^m\,, \\
\mathcal{I}_{ij}^{(n)}(t,z,\mu) &= \delta(t) I_{ij}^{(n)}(z) + \sum_{m=0}^{2n-1} \mathcal{I}_{ij}^{(n,m)}(z) \mathcal{L}_m(t,\mu^2)\,,
\end{aligned} \tag{3.5}$$

where the logarithm L_y and the distribution $\mathcal{L}_m$ are defined as

$$L_y = \ln\bigl(\mathrm{i} y \mu^2 e^{\gamma_E}\bigr)\,, \qquad \mathcal{L}_m(t,\mu^2) = \left[\frac{1}{t}\ln^m\frac{t}{\mu^2}\right]_+\,, \tag{3.6}$$

where the $[\cdots]_+$ denotes the standard plus distribution. Note that there is no one-to-one correspondence between the $\tilde{\mathcal{I}}_{ij}^{(\ell,m)}(z)$ and $\mathcal{I}_{ij}^{(\ell,m)}(z)$, as the Fourier transform induces a nontrivial mixing. For explicit relations for the Fourier transform, see e.g. ref. [106].

The logarithmic terms in eq. (3.5) encode the scale dependence of the beam function, and thus their structure is fully determined by its renormalization group equation (see appendix A.1) in terms of its anomalous dimensions and lower-order ingredients. The genuinely new three-loop results calculated by us are the nonlogarithmic boundary terms $\tilde{I}_{ij}^{(3)}(z)$ and $I_{ij}^{(3)}(z)$.

We performed several checks on our results. Firstly, we verified that all poles in ϵ cancel after applying UV renormalization and IR subtraction as given in eq. (2.8), where the beam function counterterm was predicted from its RGE as shown in appendix A.2. To check that our results obey the beam function RGE, we verified all logarithmic terms in eq. (3.5) against those predicted in ref. [33] by solving the beam function RGE. We also checked that our results for $I_{ij}(z)$ agree with the eikonal limit $\lim_{z\to 1} I_{ij}^{(3)}(z)$ that was predicted in ref. [33] using a consistency relation with the threshold soft function [29], and that our results agree with the generalized large-n_c approximation $n_c \sim n_f \gg 1$ obtained

JHEP09(2020)143

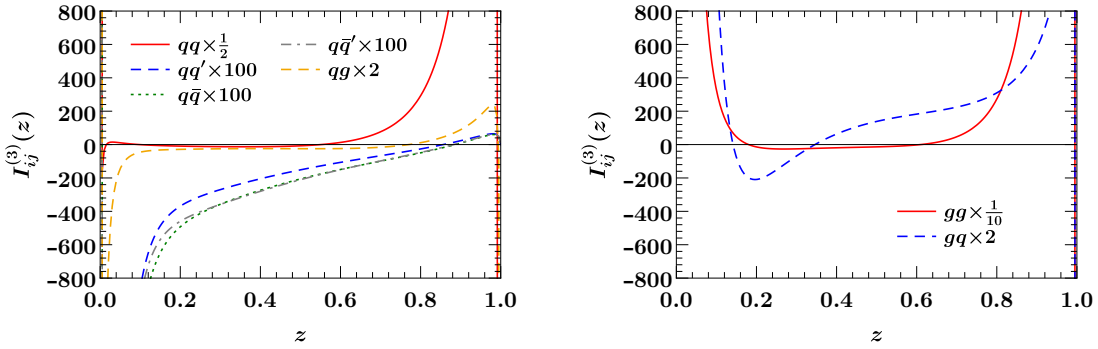

Figure 1. The N^{3}LO boundary term $I_{ij}^{(3)}$ as a function of z in all channels contributing to the quark beam function (left) and the gluon beam function (right). The different channels are rescaled as indicated in the figures.

in ref. [49]. Furthermore, we checked that the first four terms in the soft expansion of the Higgs boson production cross section reproduce correctly the collinear limit of the threshold expansion of the partonic cross section obtained for the purpose of refs. [19, 90]. The inclusive cross section at N^{3}LO for Drell-Yan and Higgs boson production was obtained in refs. [10, 11, 14, 17, 96]. We confirm that we can reproduce the first term of the threshold expansion of all partonic initial states contributing to the collinear limit of the partonic cross sections using the collinear partonic coefficient functions obtained here after integration over phase space.

To illustrate our results, figure 1 shows the beam function boundary terms $I_{ij}(z)$ relevant for the quark beam function (left) and gluon beam function (right) as a function of z. For the purpose of this plot, we replace the occurring distributions as $\delta(1-z) \to 0$ and $\mathcal{L}_n(1-z) \to \ln^n(1-z)/(1-z)$. Since the different channels give rise to very different shapes and magnitudes, they are rescaled as indicated for illustration purposes only.

To study the impact of our calculation on the beam function itself, we consider the cumulative beam function

$$B_i(t_{\text{cut}}, z, \mu) = \int_0^{t_{\text{cut}}} \mathrm{d}t\, B_i(t, z, \mu) = \sum_j \int_z^1 \frac{\mathrm{d}z'}{z'} \int_0^{t_{\text{cut}}} \mathrm{d}t\, \mathcal{I}_{ij}(t, z', \mu) f_j\left(\frac{z}{z'}, \mu\right), \tag{3.7}$$

where we distinguish both quantities only by their arguments. As indicated, this always involves the sum over all flavors j contribution the desired beam function of flavor i. We use the `MMHT2014nnlo68cl` PDF set from ref. [107] with $\alpha_s(m_Z) = 0.118$, and evaluate eq. (3.7) through an implementation of our results in `SCETlib` [108].

In figure 2, we compare the u-quark beam function (left) and gluon beam function (right) at LO (gray, dot-dashed), NLO (green, dotted), NNLO (blue, dashed) and N^{3}LO (red, solid) as a function of z. We fix $t_{\text{cut}} = (10\ \text{GeV})^2$ and $\mu = 100$ GeV and rescale the beam functions by z. Note that the LO result corresponds to the PDF itself, and thus illustrates the different shape of the beam function compared to the PDF. While we observe a notable effect of the N^{3}LO corrections, the beam functions show good convergence overall.

To judge the impact of the new three-loop boundary term $I_{ij}^{(3)}$ on resummed predictions, it is more useful to show the beam function $B_i(t_{\text{cut}}, z, \mu)$ at its canonical scale

JHEP09(2020)143

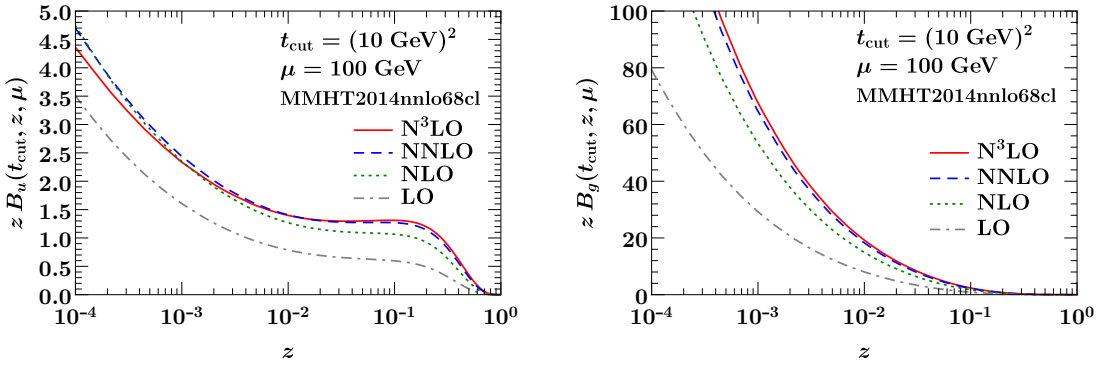

Figure 2. The cumulative u-quark (left) and the gluon (right) beam functions as a function of z for fixed $t_{\rm cut} = (10\ {\rm GeV})^2$ and $\mu = 100\ {\rm GeV}$. We show the result at LO (which corresponds to the PDF), NLO, NNLO and N^{3}LO.

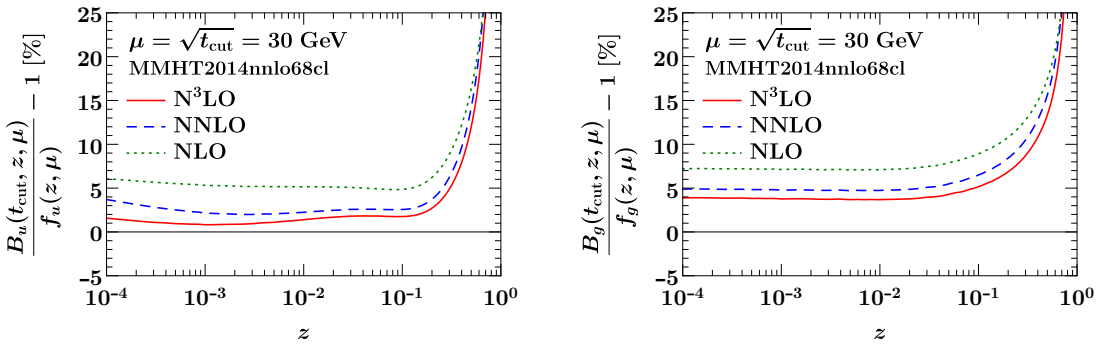

Figure 3. The relative difference of cumulative u-quark beam function (left) and the cumulative gluon beam function (right) to the corresponding PDF, as a function. We fix $\mu = \sqrt{t_{\rm cut}} = 30\ {\rm GeV}$, such that the shown beam function corresponds to the boundary term in a resummed prediction. The different colors show the results at NLO, NNLO and N^{3}LO, respectively.

$\mu = \sqrt{t_{\rm cut}}$, where all distributions $\mathcal{L}_m$ in eq. (3.5) vanish and only the boundary term $I_{ij}^{(3)}$ contributes. In figure 3, we show the cumulative beam functions at the canonical scale with $\mu = \sqrt{t_{\rm cut}} = 30\ {\rm GeV}$, showing the relative difference of the u-quark beam function (left) and the gluon beam function (right) at NLO (green, dotted), NNLO (blue, dashed) and N^{3}LO (red, solid) to the corresponding PDF itself. We observe that the shape of the beam functions differ significantly from the shape of the PDF for large z, but tend to converge towards the PDF for small $z \lesssim 10^{-1}$. As before, we see good convergence at N^{3}LO, but still a notable effect of the N^{3}LO corrections itself.

Finally, in figure 4 we show the K-factor of the N^{3}LO beam function, which we define as the ratio of the N^{3}LO beam to the NNLO beam function. As before, we choose the canonical scales $\mu = \sqrt{t_{\rm cut}} = 30\ {\rm GeV}$ as relevant for a resummed calculation, We show the K factor for u quarks (red, solid), d quarks (blue, dashed) and gluons (green, dotted). In all cases, we see corrections of $\sim 1 - 2\%$ with a sizable dependence on z.

For completeness, we also show the high-energy limit $z \to 0$ of the kernels $I_{ij}^{(3)}(z)$ in appendix B. This limit is for example interesting because the small-$\mathcal{T}_1$ region is known to grow at small z in deep inelastic scattering [109, 110].

JHEP09(2020)143

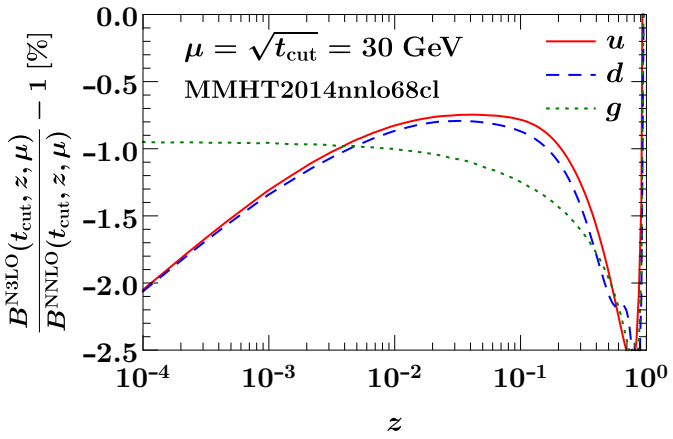

Figure 4. The K-factor of the N^{3}LO beam function, i.e. the ratio of the N^{3}LO contribution to the NNLO beam function.We fix $\mu = \sqrt{t_{\rm cut}} = 30$ GeV, such that the shown beam function corresponds to the boundary term in a resummed prediction. The different colors show the results for an u-quark, d-quark and gluon, respectively.

4 Conclusions

We have calculated the perturbative matching kernel relating N-jettiness beam functions with lightcone PDFs in all partonic channels for the first time at N^{3}LO in QCD. Our calculation is based on a method recently developed by us to expand hadronic collinear cross sections [66], demonstrating its usefulness for the calculation of universal ingredients arising in the collinear limit of QCD.

We provide our results in the form of supplementary material with this submission, where we include the renormalized N-jettiness beam function in both momentum (t) and Fourier (y) space. For the t space result, we also provide its expansions around $z = 0$ and $z = 1$ through 50 orders in the expansion.

In contrast to the TMD beam functions, which are based on the same collinear limit and at N^{3}LO can be entirely expressed in terms of harmonic polylogarithms up to weight 5 [98, 111], the $\mathcal{T}_N$ beam functions have a much richer structure of the appearing functions and are expressed in terms of Goncharov polylogarithm, as well as iterated integrals with letters that involve square roots. It will be interesting to better understand the source of this difference.

Our results have various phenomenological applications. Firstly, we provide a key ingredient to extend the N-jettiness subtraction method [30, 31] to N^{3}LO, which can be used to obtain exact fully-differential cross sections at this order. They are also crucial to extend the resummation of $\mathcal{T}_N$ to N^{3}LL$'$ and N^{4}LL accuracy, and for matching N^{3}LO calculations to parton showers based on $\mathcal{T}_0$ resummation [41, 42].

It will also be interesting to further study the collinear limit of QCD using the underlying method of collinear expansions. In particular, we expect this to shed light on the universal structure of $\mathcal{T}_N$ factorization at subleading power [112–120], which has recently attracted much attention in the literature due to its importance for $\mathcal{T}_N$-subtractions [34–40, 121].

JHEP09(2020)143

Acknowledgments

We thank Johannes Michel, Iain Stewart and Frank Tackmann for useful discussions. This work was supported by the Office of Nuclear Physics of the U.S. Department of Energy under Contract No. DE-SC0011090 and DE-AC02-76SF00515. M.E. is also supported by the Alexander von Humboldt Foundation through a Feodor Lynen Research Fellowship, and B.M. is also supported by a Pappalardo fellowship.

A Ingredients for the calculation of the beam function

In this appendix, we provide more details on the regularization and renormalization of the beam function kernels. Details of the calculation of all required integrals will be presented in ref. [99].

A.1 Renormalization group equations

In t space, the beam function $B_i(t,z,\mu)$ obeys the RGE [20, 43]

$$\mu\frac{\mathrm{d}}{\mathrm{d}\mu}B_i(t,z,\mu) = \int \mathrm{d}t'\,\gamma_B^i(t-t',\mu)\,B_i(t',z,\mu)\,, \tag{A.1}$$

where the anomalous dimension γ_B^i has the all-order form

$$\gamma_B^i(t,\mu) = -2\Gamma^i_{\mathrm{cusp}}[\alpha_s(\mu)]\,\mathcal{L}_0(t,\mu^2) + \gamma_B^i[\alpha_s(\mu)]\,\delta(t)\,. \tag{A.2}$$

Here, $\Gamma^i_{\mathrm{cusp}}(\alpha_s)$ and $\gamma_B^i(\alpha_s)$ are the cusp and beam noncusp anomalous dimensions, which both depend on the color representation $i = q$ or $i = g$ only, but are independent of the quark flavor. The RGE for the matching kernel follows from eqs. (2.6) and (A.1) and the DGLAP equation

$$\mu\frac{\mathrm{d}}{\mathrm{d}\mu}f_i(z,\mu) = 2\sum_j\int_z^1\frac{\mathrm{d}z'}{z'}\,P_{ij}(z',\mu)\,f_j\biggl(\frac{z}{z'},\mu\biggr)\,. \tag{A.3}$$

It is given by [43]

$$\begin{aligned}\mu\frac{\mathrm{d}}{\mathrm{d}\mu}\mathcal{I}_{ij}(t,z,\mu) = \sum_k\int\mathrm{d}t'\int_z^1\frac{\mathrm{d}z'}{z'}\,\mathcal{I}_{ik}\biggl(t-t',\frac{z}{z'},\mu\biggr)\\ \times\Bigl[\gamma_B^i(t',\mu)\,\delta_{kj}\delta(1-z') - \delta(t')\,2P_{kj}(z',\mu)\Bigr]\,.\end{aligned} \tag{A.4}$$

A.2 Structure of the beam function counterterm

We define the Fourier transformation of a function f as

$$\tilde f(y,\cdots) = \int\mathrm{d}t\,e^{-\mathrm{i}ty}\,f(t,\cdots)\,,\qquad f(t,\cdots) = \int\frac{\mathrm{d}y}{2\pi}\,e^{\mathrm{i}ty}\,\tilde f(y,\cdots)\,. \tag{A.5}$$

The Fourier transform of the bare kernel $\mathcal{I}_{ij}(t,z,\epsilon)$ can be conveniently evaluated using

$$\mu^{2a\epsilon}\int_{-\infty}^{\infty}\mathrm{d}t\,e^{-\mathrm{i}ty}\frac{\theta(t)}{t^{1+a\epsilon}} = e^{a\epsilon(L_y-\gamma_E)}\Gamma(-a\epsilon)\,,\qquad L_y = \ln\bigl(\mathrm{i}y\mu^2e^{\gamma_E}\bigr)\,. \tag{A.6}$$

JHEP09(2020)143

Here, L_y is the canonical logarithm in Fourier space, and γ_E is the Euler-Mascheroni constant. In Fourier space, the renormalization of the bare matching kernel in eq. (2.8) becomes multiplicative in y,

$$\tilde{\mathcal{I}}_{ij}(y,z,\mu) = \sum_k \int_z^1 \frac{\mathrm{d}z'}{z'}\, \Gamma_{jk}\!\left(\frac{z}{z'},\epsilon\right) \tilde{Z}_B^i(y,\epsilon,\mu)\hat{Z}_{\alpha_s}(\mu,\epsilon)\,\tilde{\mathcal{I}}_{ik}(y,z',\epsilon)\,, \tag{A.7}$$

and the counterterm $\tilde{Z}_B^i$ follows from the RG eq. (A.2) in y space,

$$\begin{aligned}\frac{\mathrm{d}}{\mathrm{d}\ln\mu}\ln\tilde{B}_i(y,z,\mu) = \tilde{\gamma}_B^i(y,\mu) &= -\frac{\mathrm{d}}{\mathrm{d}\ln\mu}\ln\tilde{Z}_B^i(y,\mu,\epsilon) \\ &= 2\Gamma^i_{\mathrm{cusp}}[\alpha_s(\mu)]L_y + \gamma_B^i[\alpha_s(\mu)]\,. \end{aligned}\tag{A.8}$$

Solving eq. (A.8), we can predict the all-order pole structure of $\tilde{Z}_B^i$ as (see also ref. [122])

$$\ln\tilde{Z}_i^B(y,\mu,\epsilon) = -\int_0^{\alpha_s(\mu)} \frac{\mathrm{d}\alpha}{\beta(\alpha,\epsilon)}\left[4\Gamma^i_{\mathrm{cusp}}(\alpha)\int_{\alpha_s(\mu)}^{\alpha}\frac{\mathrm{d}\alpha'}{\beta(\alpha',\epsilon)} + 2\Gamma^i_{\mathrm{cusp}}(\alpha)L_y + \gamma_B^i(\alpha)\right], \tag{A.9}$$

where $\beta(\alpha_s,\epsilon) = -2\epsilon\alpha_s + \beta(\alpha_s)$ is the QCD beta function in $d = 4-2\epsilon$ dimensions. Expanding eq. (A.9) systematically in α, we obtain the result through three loops as

$$\begin{aligned}\ln\tilde{Z}_i^B(y,\mu,\epsilon) = {}& \frac{\alpha_s}{4\pi}\left\{\frac{\Gamma_0^i}{\epsilon^2} + \frac{1}{2\epsilon}\big(2\Gamma_0^i L_y + \gamma_{B\,0}^i\big)\right\} \\ &+ \left(\frac{\alpha_s}{4\pi}\right)^2\left\{-\frac{3}{4}\frac{\beta_0\Gamma_0^i}{\epsilon^3} - \frac{1}{4\epsilon^2}\big[\beta_0\big(2\Gamma_0^i L_y + \gamma_{B\,0}^i\big) - \Gamma_1^i\big] + \frac{1}{4\epsilon}\big(2\Gamma_1^i L_y + \gamma_{B\,1}^i\big)\right\} \\ &+ \left(\frac{\alpha_s}{4\pi}\right)^3\left\{\frac{11}{18}\frac{\beta_0^2\Gamma_0^i}{\epsilon^4} + \frac{1}{6\epsilon^3}\left[\beta_0^2\big(2\Gamma_0^i L_y + \gamma_{B\,0}^i\big) - \frac{5}{3}\beta_0\Gamma_1^i - \frac{8}{3}\beta_1\Gamma_0^i\right]\right. \\ &\qquad - \frac{1}{6\epsilon^2}\left[\beta_1\big(2\Gamma_0^i L_y + \gamma_{B\,0}^i\big) + \beta_0\big(2\Gamma_1^i L_y + \gamma_{B\,1}^i\big) - \frac{2}{3}\Gamma_2^i\right] \\ &\qquad \left. + \frac{1}{6\epsilon}\big(2\Gamma_2^i L_y + \gamma_{B\,2}^i\big)\right\} + \mathcal{O}(\alpha_s^4)\,. \end{aligned}\tag{A.10}$$

Here, the γ_n are the coefficients of the corresponding anomalous dimensions at $\mathcal{O}[(\alpha_s/4\pi)^n]$. Explicit expressions for all anomalous dimensions in the convention of eq. (A.10) are collected in ref. [33]. The required three-loop results for Γ_{cusp} and β were calculated in refs. [123–125] and refs. [126, 127], respectively. The beam noncusp anomalous dimension were originally determined in refs. [43, 44], see also refs. [64, 65].

A.3 α_s renormalization and IR counterterms

The bare strong coupling constant is renormalised as

$$\begin{aligned}\alpha_s^b = \alpha_s\left(\frac{\mu^2}{4\pi}e^{\gamma_E}\right)^{\epsilon}\left[1 + \frac{\alpha_s}{4\pi}\left(-\frac{\beta_0}{\epsilon}\right) + \left(\frac{\alpha_s}{4\pi}\right)^2\left(\frac{\beta_0^2}{\epsilon^2} - \frac{\beta_1}{2\epsilon}\right)\right. \\ \left. + \left(\frac{\alpha_s}{4\pi}\right)^3\left(-\frac{\beta_0^3}{\epsilon^3} + \frac{7\beta_1\beta_0}{6\epsilon^2} - \frac{\beta_2}{3\epsilon}\right) + \mathcal{O}(\alpha_s^4)\right]. \end{aligned}\tag{A.11}$$

JHEP09(2020)143

The mass factorisation counter term can be expressed in terms of the splitting functions P_{ij} [124, 125] as

$$\begin{aligned}\Gamma_{ij}(z) = \;& \delta_{ij}\delta(1-z) \\ & + \left(\frac{\alpha_s}{4\pi}\right)\frac{P_{ij}^{(0)}}{\epsilon} \\ & + \left(\frac{\alpha_s}{4\pi}\right)^2\left[\frac{1}{2\epsilon^2}\left(P_{ik}^{(0)}\otimes P_{kj}^{(0)} - \beta_0 P_{ij}^{(0)}\right) + \frac{1}{2\epsilon}P_{kj}^{(1)}\right] \\ & + \left(\frac{\alpha_s}{4\pi}\right)^3\left[\frac{1}{6\epsilon^3}\left(P_{ik}^{(0)}\otimes P_{kl}^{(0)}\otimes P_{lj}^{(0)} - 3\beta_0 P_{ik}^{(0)}\otimes P_{kj}^{(0)} + 2\beta_0^2 P_{ij}^{(0)}\right)\right. \\ & \qquad \left. + \frac{1}{6\epsilon^2}\left(P_{ik}^{(1)}\otimes P_{kj}^{(0)} + 2P_{ik}^{(0)}\otimes P_{kj}^{(1)} - 2\beta_0 P_{ij}^{(1)} - 2\beta_1 P_{ij}^{(0)}\right) + \frac{1}{3\epsilon}P_{ij}^{(2)}\right]. \\ & + \mathcal{O}(\alpha_s^4)\,. \end{aligned} \tag{A.12}$$

Here, we suppress the argument z of the splitting functions on the right hand side and keep the summation over repeated flavor indices implicit. The convolution in eq. (A.12) is defined as

$$f\otimes g = \int_z^1 \frac{\mathrm{d}z'}{z'} f(z) g\left(\frac{z}{z'}\right). \tag{A.13}$$

B High-energy limit of the beam function kernels

Here, we present the high-energy limit $z\to 0$ of the beam function $I_{ij}^{(3)}(z)$:

$$\begin{aligned}\lim_{z\to 0} z\, I_{gg}^{(3)}(z) = \;& -\frac{1}{120}C_A^3\ln^5(z) + \ln^4(z)\left(\frac{11C_A^3}{72} - \frac{C_A^2 n_f}{72} - \frac{C_A C_F n_f}{72}\right) \\ & + \ln^3(z)\left[C_A^3\left(-\frac{\zeta_2}{4} - \frac{229}{216}\right) + \frac{17C_A^2 n_f}{54} + C_A\left(\frac{C_F n_f}{6} - \frac{n_f^2}{108}\right) - \frac{C_F n_f^2}{27}\right] \\ & + \ln^2(z)\left[C_A^3\left(\frac{143\zeta_2}{16} - \frac{25\zeta_3}{24} - \frac{1013}{96}\right) + C_A^2 n_f\left(\frac{1207}{432} - \frac{17\zeta_2}{24}\right)\right. \\ & \qquad + C_A\left(C_F n_f\left(\frac{745}{864} - \frac{3\zeta_2}{4}\right) - \frac{23n_f^2}{216}\right) \\ & \qquad \left. + C_F^2 n_f\left(\frac{11}{48} - \frac{\zeta_2}{6}\right) - \frac{5C_F n_f^2}{27}\right] \\ & + \ln(z)\left[C_A^3\left(\frac{15143\zeta_2}{432} + \frac{407\zeta_3}{36} - \frac{1433\zeta_4}{48} - \frac{43393}{2592}\right)\right. \\ & \qquad + C_F n_f^2\left(\frac{\zeta_2}{9} - \frac{25}{81}\right) + C_A C_F n_f\left(-\frac{377}{216}\zeta_2 - \frac{22\zeta_3}{9} + \frac{5033}{3888}\right) \\ & \qquad + C_A n_f^2\left(\frac{\zeta_2}{18} - \frac{251}{648}\right) + C_F^2 n_f\left(\frac{311}{288} - \frac{25\zeta_2}{36}\right) \\ & \qquad \left. + C_A^2 n_f\left(-\frac{1031}{216}\zeta_2 - \frac{\zeta_3}{18} + \frac{11027}{1296}\right)\right] \\ & + \mathcal{O}(\ln^0 z)\,, \end{aligned} \tag{B.1}$$

JHEP09(2020)143

$$\begin{aligned}
\lim_{z\to 0} z\, I_{gq}^{(3)}(z) = &-\frac{1}{120}C_A^2 C_F \ln^5(z) + \ln^4(z)\left(\frac{5C_A^2C_F}{36} - \frac{C_A C_F n_f}{36} + \frac{C_F^2 n_f}{72}\right)\\
&+\ln^3(z)\left[C_A^2C_F\left(\frac{\zeta_2}{12} - \frac{89}{72}\right) + C_A C_F^2\left(\frac{5}{24} - \frac{\zeta_2}{3}\right)\right.\\
&\qquad\left. + C_A C_F n_f \frac{97}{216} - \frac{C_F^2 n_f}{54} - \frac{C_F n_f^2}{36}\right]\\
&+\ln^2(z)\left[C_A^2C_F\left(\frac{103\zeta_2}{16} - \frac{7\zeta_3}{24} - \frac{83}{9}\right) + C_A C_F^2\left(\frac{73\zeta_2}{24} - \frac{5\zeta_3}{4} - \frac{151}{96}\right)\right.\\
&\qquad - \frac{5C_F n_f^2}{36} + C_A C_F n_f\left(\frac{2275}{864} - \frac{2\zeta_2}{3}\right) + C_F^3\left(-\frac{3\zeta_2}{4} + \frac{\zeta_3}{2} + \frac{13}{16}\right)\\
&\qquad\left. + C_F^2 n_f\left(\frac{157}{432} - \frac{3\zeta_2}{4}\right)\right]\\
&+\ln(z)\left[C_F^3\left(-\frac{19}{8}\zeta_2 + \frac{3\zeta_3}{2} - 5\zeta_4 + \frac{93}{16}\right)\right.\\
&\qquad + C_A C_F n_f\left(-\frac{265}{108}\zeta_2 - \frac{\zeta_3}{6} + \frac{1619}{324}\right)\\
&\qquad + C_F^2 n_f\left(-\frac{193}{108}\zeta_2 - \frac{37\zeta_3}{18} + \frac{24757}{7776}\right)\\
&\qquad + C_A C_F^2\left(\frac{757\zeta_2}{48} - \frac{9\zeta_3}{4} - \frac{45\zeta_4}{8} - \frac{3055}{192}\right)\\
&\qquad\left. + C_A^2 C_F\left(\frac{2099\zeta_2}{108} + \frac{106\zeta_3}{9} - \frac{923\zeta_4}{48} - \frac{3377}{576}\right) - \frac{25C_F n_f^2}{108}\right]\\
&+\mathcal{O}(\ln^0 z)\,, \qquad \text{(B.2)}\\
\lim_{z\to 0} z\, I_{qg}^{(3)}(z) = &\, C_A^2\left(\frac{2\zeta_3}{9} - \frac{322}{243}\right)\ln(z)\\
&+C_A^2\left(-\frac{1}{324}337\zeta_2 + \frac{787\zeta_3}{432} + \frac{263\zeta_4}{144} - \frac{266675}{23328}\right) + C_A n_f\left(-\frac{\zeta_3}{27} - \frac{1169}{23328}\right)\\
&+C_A C_F\left(-\frac{\zeta_2}{108} - \frac{7\zeta_4}{6} - \frac{\zeta_3}{12} - \frac{1103}{1728}\right) + C_F n_f\left(\frac{6049}{11664} - \frac{2\zeta_3}{27}\right)\,, \qquad \text{(B.3)}\\
\lim_{z\to 0} z\, I_{qq}^{(3)}(z) = &\lim_{z\to 0} z\, I_{q\bar{q}}^{(3)}(z) = \lim_{z\to 0} z\, I_{qq'}^{(3)}(z) = \lim_{z\to 0} z\, I_{q\bar{q}'}^{(3)}(z)\\
= &\, C_A C_F\left(\frac{2\zeta_3}{9} - \frac{322}{243}\right)\ln(z) + C_F^2\left(-\frac{\zeta_2}{108} - \frac{7\zeta_4}{6} - \frac{\zeta_3}{12} - \frac{1103}{1728}\right)\\
&+C_F n_f\left(\frac{305}{1458} - \frac{2\zeta_3}{27}\right) + C_A C_F\left(-\frac{337}{324}\zeta_2 + \frac{257\zeta_3}{144} + \frac{263\zeta_4}{144} - \frac{258211}{23328}\right).\\
&\qquad \text{(B.4)}
\end{aligned}$$

Here, the color factors C_A and C_F are only used for compactness of the result and should be replaced with their expressions in terms of n_c. Note that the expressions for the high energy limit $z \to 0$ up to $\mathcal{O}(z^{50})$, as well as that for the threshold limit $z \to 1$ up to $\mathcal{O}((1-z)^{50})$, can be found in electronic form in the supplementary material.

JHEP09(2020)143

References

[1] ATLAS collaboration, *Measurement of the W-boson mass in pp collisions at $\sqrt{s} = 7$ TeV with the ATLAS detector*, *Eur. Phys. J. C* **78** (2018) 110 [*Erratum ibid.* **78** (2018) 898] [arXiv:1701.07240] [INSPIRE].

[2] ATLAS collaboration, *Measurement of the Drell-Yan triple-differential cross section in pp collisions at $\sqrt{s} = 8$ TeV*, *JHEP* **12** (2017) 059 [arXiv:1710.05167] [INSPIRE].

[3] CMS collaboration, *Measurement of the transverse momentum spectra of weak vector bosons produced in proton-proton collisions at $\sqrt{s} = 8$ TeV*, *JHEP* **02** (2017) 096 [arXiv:1606.05864] [INSPIRE].

[4] CMS collaboration, *Measurements of differential Z boson production cross sections in proton-proton collisions at $\sqrt{s} = 13$ TeV*, *JHEP* **12** (2019) 061 [arXiv:1909.04133] [INSPIRE].

[5] CMS collaboration, *Combined measurements of Higgs boson couplings in proton-proton collisions at $\sqrt{s} = 13$ TeV*, *Eur. Phys. J. C* **79** (2019) 421 [arXiv:1809.10733] [INSPIRE].

[6] ATLAS collaboration, *Higgs boson production cross-section measurements and their EFT interpretation in the 4ℓ decay channel at $\sqrt{s} = 13$ TeV with the ATLAS detector*, arXiv:2004.03447 [INSPIRE].

[7] ATLAS collaboration, *Measurement of fiducial and differential W^+W^- production cross-sections at $\sqrt{s} = 13$ TeV with the ATLAS detector*, *Eur. Phys. J. C* **79** (2019) 884 [arXiv:1905.04242] [INSPIRE].

[8] ATLAS collaboration, *Measurement of ZZ production in the $\ell\ell\nu\nu$ final state with the ATLAS detector in pp collisions at $\sqrt{s} = 13$ TeV*, *JHEP* **10** (2019) 127 [arXiv:1905.07163] [INSPIRE].

[9] CMS collaboration, *Search for anomalous triple gauge couplings in WW and WZ production in lepton + jet events in proton-proton collisions at $\sqrt{s} = 13$ TeV*, *JHEP* **12** (2019) 062 [arXiv:1907.08354] [INSPIRE].

[10] C. Anastasiou et al., *Higgs boson gluon-fusion production at threshold in N^3LO QCD*, *Phys. Lett. B* **737** (2014) 325 [arXiv:1403.4616] [INSPIRE].

[11] C. Anastasiou, C. Duhr, F. Dulat, F. Herzog and B. Mistlberger, *Higgs boson gluon-fusion production in QCD at three loops*, *Phys. Rev. Lett.* **114** (2015) 212001 [arXiv:1503.06056] [INSPIRE].

[12] F.A. Dreyer and A. Karlberg, *Vector-boson fusion Higgs production at three loops in QCD*, *Phys. Rev. Lett.* **117** (2016) 072001 [arXiv:1606.00840] [INSPIRE].

[13] F.A. Dreyer and A. Karlberg, *Vector-boson fusion Higgs pair production at N^3LO*, *Phys. Rev. D* **98** (2018) 114016 [arXiv:1811.07906] [INSPIRE].

[14] B. Mistlberger, *Higgs boson production at hadron colliders at N^3LO in QCD*, *JHEP* **05** (2018) 028 [arXiv:1802.00833] [INSPIRE].

JHEP09(2020)143

[15] C. Duhr, F. Dulat and B. Mistlberger, *Higgs production in bottom-quark fusion to third order in the strong coupling*, *Phys. Rev. Lett.* **125** (2020) 051804 [arXiv:1904.09990] [INSPIRE].

[16] C. Duhr, F. Dulat, V. Hirschi and B. Mistlberger, *Higgs production in bottom quark fusion: matching the 4- and 5-flavour schemes to third order in the strong coupling*, *JHEP* **08** (2020) 017 [arXiv:2004.04752] [INSPIRE].

[17] C. Duhr, F. Dulat and B. Mistlberger, *The Drell-Yan cross section to third order in the strong coupling constant*, arXiv:2001.07717 [INSPIRE].

[18] L. Cieri, X. Chen, T. Gehrmann, E.W.N. Glover and A. Huss, *Higgs boson production at the LHC using the q_T subtraction formalism at N^3LO QCD*, *JHEP* **02** (2019) 096 [arXiv:1807.11501] [INSPIRE].

[19] F. Dulat, B. Mistlberger and A. Pelloni, *Precision predictions at N^3LO for the Higgs boson rapidity distribution at the LHC*, *Phys. Rev. D* **99** (2019) 034004 [arXiv:1810.09462] [INSPIRE].

[20] I.W. Stewart, F.J. Tackmann and W.J. Waalewijn, *Factorization at the LHC: from PDFs to initial state jets*, *Phys. Rev. D* **81** (2010) 094035 [arXiv:0910.0467] [INSPIRE].

[21] I.W. Stewart, F.J. Tackmann and W.J. Waalewijn, *N-jettiness: an inclusive event shape to veto jets*, *Phys. Rev. Lett.* **105** (2010) 092002 [arXiv:1004.2489] [INSPIRE].

[22] I.W. Stewart, F.J. Tackmann and W.J. Waalewijn, *The beam thrust cross section for Drell-Yan at NNLL order*, *Phys. Rev. Lett.* **106** (2011) 032001 [arXiv:1005.4060] [INSPIRE].

[23] T.T. Jouttenus, I.W. Stewart, F.J. Tackmann and W.J. Waalewijn, *The soft function for exclusive N-jet production at hadron colliders*, *Phys. Rev. D* **83** (2011) 114030 [arXiv:1102.4344] [INSPIRE].

[24] C.W. Bauer, S. Fleming and M.E. Luke, *Summing Sudakov logarithms in $B \to X(s\gamma)$ in effective field theory*, *Phys. Rev. D* **63** (2000) 014006 [hep-ph/0005275] [INSPIRE].

[25] C.W. Bauer, S. Fleming, D. Pirjol and I.W. Stewart, *An effective field theory for collinear and soft gluons: heavy to light decays*, *Phys. Rev. D* **63** (2001) 114020 [hep-ph/0011336] [INSPIRE].

[26] C.W. Bauer and I.W. Stewart, *Invariant operators in collinear effective theory*, *Phys. Lett. B* **516** (2001) 134 [hep-ph/0107001] [INSPIRE].

[27] C.W. Bauer, D. Pirjol and I.W. Stewart, *Soft collinear factorization in effective field theory*, *Phys. Rev. D* **65** (2002) 054022 [hep-ph/0109045] [INSPIRE].

[28] C.W. Bauer, S. Fleming, D. Pirjol, I.Z. Rothstein and I.W. Stewart, *Hard scattering factorization from effective field theory*, *Phys. Rev. D* **66** (2002) 014017 [hep-ph/0202088] [INSPIRE].

[29] G. Lustermans, J.K.L. Michel and F.J. Tackmann, *Generalized threshold factorization with full collinear dynamics*, arXiv:1908.00985 [INSPIRE].

[30] R. Boughezal, C. Focke, X. Liu and F. Petriello, *W-boson production in association with a jet at next-to-next-to-leading order in perturbative QCD*, *Phys. Rev. Lett.* **115** (2015) 062002 [arXiv:1504.02131] [INSPIRE].

JHEP09(2020)143

[31] J. Gaunt, M. Stahlhofen, F.J. Tackmann and J.R. Walsh, *N-jettiness Subtractions for NNLO QCD Calculations*, *JHEP* **09** (2015) 058 [arXiv:1505.04794] [INSPIRE].

[32] S. Catani and M. Grazzini, *An NNLO subtraction formalism in hadron collisions and its application to Higgs boson production at the LHC*, *Phys. Rev. Lett.* **98** (2007) 222002 [hep-ph/0703012] [INSPIRE].

[33] G. Billis, M.A. Ebert, J.K.L. Michel and F.J. Tackmann, *A toolbox for q_T and 0-jettiness subtractions at N^3LO*, arXiv:1909.00811 [INSPIRE].

[34] I. Moult, L. Rothen, I.W. Stewart, F.J. Tackmann and H.X. Zhu, *Subleading power corrections for N-jettiness subtractions*, *Phys. Rev. D* **95** (2017) 074023 [arXiv:1612.00450] [INSPIRE].

[35] I. Moult, L. Rothen, I.W. Stewart, F.J. Tackmann and H.X. Zhu, *N-jettiness subtractions for $gg \to H$ at subleading power*, *Phys. Rev. D* **97** (2018) 014013 [arXiv:1710.03227] [INSPIRE].

[36] M.A. Ebert, I. Moult, I.W. Stewart, F.J. Tackmann, G. Vita and H.X. Zhu, *Power corrections for N-jettiness subtractions at $\mathcal{O}(\alpha_s)$*, *JHEP* **12** (2018) 084 [arXiv:1807.10764] [INSPIRE].

[37] R. Boughezal, X. Liu and F. Petriello, *Power corrections in the N-jettiness subtraction scheme*, *JHEP* **03** (2017) 160 [arXiv:1612.02911] [INSPIRE].

[38] R. Boughezal, A. Isgrò and F. Petriello, *Next-to-leading-logarithmic power corrections for N-jettiness subtraction in color-singlet production*, *Phys. Rev. D* **97** (2018) 076006 [arXiv:1802.00456] [INSPIRE].

[39] R. Boughezal, A. Isgrò and F. Petriello, *Next-to-leading power corrections to $V+1$ jet production in N-jettiness subtraction*, *Phys. Rev. D* **101** (2020) 016005 [arXiv:1907.12213] [INSPIRE].

[40] M.A. Ebert and F.J. Tackmann, *Impact of isolation and fiducial cuts on q_T and N-jettiness subtractions*, *JHEP* **03** (2020) 158 [arXiv:1911.08486] [INSPIRE].

[41] S. Alioli et al., *Combining higher-order resummation with multiple NLO calculations and parton showers in GENEVA*, *JHEP* **09** (2013) 120 [arXiv:1211.7049] [INSPIRE].

[42] S. Alioli, C.W. Bauer, C. Berggren, F.J. Tackmann and J.R. Walsh, *Drell-Yan production at NNLL'+NNLO matched to parton showers*, *Phys. Rev. D* **92** (2015) 094020 [arXiv:1508.01475] [INSPIRE].

[43] I.W. Stewart, F.J. Tackmann and W.J. Waalewijn, *The quark beam function at NNLL*, *JHEP* **09** (2010) 005 [arXiv:1002.2213] [INSPIRE].

[44] C.F. Berger, C. Marcantonini, I.W. Stewart, F.J. Tackmann and W.J. Waalewijn, *Higgs production with a central jet veto at NNLL+NNLO*, *JHEP* **04** (2011) 092 [arXiv:1012.4480] [INSPIRE].

[45] J.R. Gaunt, M. Stahlhofen and F.J. Tackmann, *The quark beam function at two loops*, *JHEP* **04** (2014) 113 [arXiv:1401.5478] [INSPIRE].

[46] J. Gaunt, M. Stahlhofen and F.J. Tackmann, *The gluon beam function at two loops*, *JHEP* **08** (2014) 020 [arXiv:1405.1044] [INSPIRE].

[47] K. Melnikov, R. Rietkerk, L. Tancredi and C. Wever, *Double-real contribution to the quark beam function at N^3LO QCD*, *JHEP* **02** (2019) 159 [arXiv:1809.06300] [INSPIRE].

JHEP09(2020)143

[48] K. Melnikov, R. Rietkerk, L. Tancredi and C. Wever, *Triple-real contribution to the quark beam function in QCD at next-to-next-to-next-to-leading order*, *JHEP* **06** (2019) 033 [arXiv:1904.02433] [INSPIRE].

[49] A. Behring, K. Melnikov, R. Rietkerk, L. Tancredi and C. Wever, *Quark beam function at next-to-next-to-next-to-leading order in perturbative QCD in the generalized large-N_c approximation*, *Phys. Rev. D* **100** (2019) 114034 [arXiv:1910.10059] [INSPIRE].

[50] M.D. Schwartz, *Resummation and NLO matching of event shapes with effective field theory*, *Phys. Rev. D* **77** (2008) 014026 [arXiv:0709.2709] [INSPIRE].

[51] S. Fleming, A.H. Hoang, S. Mantry and I.W. Stewart, *Top jets in the peak region: factorization analysis with NLL resummation*, *Phys. Rev. D* **77** (2008) 114003 [arXiv:0711.2079] [INSPIRE].

[52] R. Kelley, M.D. Schwartz, R.M. Schabinger and H.X. Zhu, *The two-loop hemisphere soft function*, *Phys. Rev. D* **84** (2011) 045022 [arXiv:1105.3676] [INSPIRE].

[53] P.F. Monni, T. Gehrmann and G. Luisoni, *Two-loop soft corrections and resummation of the thrust distribution in the dijet region*, *JHEP* **08** (2011) 010 [arXiv:1105.4560] [INSPIRE].

[54] A. Hornig, C. Lee, I.W. Stewart, J.R. Walsh and S. Zuberi, *Non-global structure of the $O(\alpha_s^2)$ dijet soft function*, *JHEP* **08** (2011) 054 [*Erratum ibid.* **10** (2017) 101] [arXiv:1105.4628] [INSPIRE].

[55] R. Boughezal, X. Liu and F. Petriello, *N-jettiness soft function at next-to-next-to-leading order*, *Phys. Rev. D* **91** (2015) 094035 [arXiv:1504.02540] [INSPIRE].

[56] J.M. Campbell, R.K. Ellis, R. Mondini and C. Williams, *The NNLO QCD soft function for 1-jettiness*, *Eur. Phys. J. C* **78** (2018) 234 [arXiv:1711.09984] [INSPIRE].

[57] G. Bell, B. Dehnadi, T. Mohrmann and R. Rahn, *Automated calculation of $\boldsymbol{N}$-jet soft functions*, PoS(LL2018)044 [arXiv:1808.07427] [INSPIRE].

[58] S. Jin and X. Liu, *Two-loop N-jettiness soft function for $pp \to 2j$ production*, *Phys. Rev. D* **99** (2019) 114017 [arXiv:1901.10935] [INSPIRE].

[59] C.W. Bauer and A.V. Manohar, *Shape function effects in $B \to X(s)\gamma$ and $B \to X(u)l\bar{\nu}$ decays*, *Phys. Rev. D* **70** (2004) 034024 [hep-ph/0312109] [INSPIRE].

[60] T. Becher and M. Neubert, *Toward a NNLO calculation of the $\bar{B} \to X(s)\gamma$ decay rate with a cut on photon energy. II. Two-loop result for the jet function*, *Phys. Lett. B* **637** (2006) 251 [hep-ph/0603140] [INSPIRE].

[61] S. Fleming, A.K. Leibovich and T. Mehen, *Resumming the color octet contribution to $e^+e^- \to J/\psi + X$*, *Phys. Rev. D* **68** (2003) 094011 [hep-ph/0306139] [INSPIRE].

[62] T. Becher and M.D. Schwartz, *Direct photon production with effective field theory*, *JHEP* **02** (2010) 040 [arXiv:0911.0681] [INSPIRE].

[63] T. Becher and G. Bell, *The gluon jet function at two-loop order*, *Phys. Lett. B* **695** (2011) 252 [arXiv:1008.1936] [INSPIRE].

[64] R. Brüser, Z. L. Liu and M. Stahlhofen, *Three-loop quark jet function*, *Phys. Rev. Lett.* **121** (2018) 072003 [arXiv:1804.09722] [INSPIRE].

[65] P. Banerjee, P.K. Dhani and V. Ravindran, *Gluon jet function at three loops in QCD*, *Phys. Rev. D* **98** (2018) 094016 [arXiv:1805.02637] [INSPIRE].

JHEP09(2020)143

[66] M.A. Ebert, B. Mistlberger and G. Vita, *Collinear expansion for color singlet cross sections*, arXiv:2006.03055 [INSPIRE].

[67] C. Anastasiou and K. Melnikov, *Pseudoscalar Higgs boson production at hadron colliders in next-to-next-to-leading order QCD*, *Phys. Rev. D* **67** (2003) 037501.

[68] C. Anastasiou, L.J. Dixon and K. Melnikov, *NLO Higgs boson rapidity distributions at hadron colliders*, *Nucl. Phys. B Proc. Suppl.* **116** (2003) 193 [hep-ph/0211141] [INSPIRE].

[69] C. Anastasiou, L. Dixon, K. Melnikov and F. Petriello, *Dilepton rapidity distribution in the Drell-Yan process at next-to-next-to-leading order in QCD*, *Phys. Rev. Lett.* **91** (2003) 182002.

[70] C. Anastasiou, K. Melnikov and F. Petriello, *Fully differential Higgs boson production and the di-photon signal through next-to-next-to-leading order*, *Nucl. Phys. B* **724** (2005) 197.

[71] C. Anastasiou, L. Dixon, K. Melnikov and F. Petriello, *High-precision QCD at hadron colliders: Electroweak gauge boson rapidity distributions at next-to-next-to leading order*, *Phys. Rev. D.* **69** (2004) 094008

[72] K.G. Chetyrkin and F.V. Tkachov, *Integration by parts: the algorithm to calculate β-functions in 4 loops*, *Nucl. Phys. B* **192** (1981) 159 [INSPIRE].

[73] F.V. Tkachov, *A theorem on analytical calculability of four loop renormalization group functions*, *Phys. Lett. B* **100** (1981) 65 [INSPIRE].

[74] A.V. Kotikov, *Differential equations method: new technique for massive Feynman diagrams calculation*, *Phys. Lett. B* **254** (1991) 158 [INSPIRE].

[75] A.V. Kotikov, *Differential equations method: the calculation of vertex type Feynman diagrams*, *Phys. Lett. B* **259** (1991) 314 [INSPIRE].

[76] A.V. Kotikov, *Differential equation method: the calculation of N point Feynman diagrams*, *Phys. Lett. B* **267** (1991) 123 [*Erratum ibid.* **295** (1992) 409] [INSPIRE].

[77] J.M. Henn, *Multiloop integrals in dimensional regularization made simple*, *Phys. Rev. Lett.* **110** (2013) 251601 [arXiv:1304.1806] [INSPIRE].

[78] T. Gehrmann and E. Remiddi, *Differential equations for two loop four point functions*, *Nucl. Phys. B* **580** (2000) 485 [hep-ph/9912329] [INSPIRE].

[79] T. Inami, T. Kubota and Y. Okada, *Effective gauge theory and the effect of heavy quarks*, *Z. Phys. C* **18** (1983) 69

[80] M. Shifman, A. Vainshtein and V. Zakharov, *Remarks on Higgs-boson interactions with nucleons*, *Phys. Lett. B* **78** (1978) 443

[81] V.P. Spiridonov and K.G. Chetyrkin, *Nonleading mass corrections and renormalization of the operators $m\bar{\psi}$ and $g^2(\mu\nu)$*, *Sov. J. Nucl. Phys.* **47** (1988) 522 [*Yad. Fiz.* **47** (1988) 818] [INSPIRE].

[82] F. Wilczek, *Decays of heavy vector mesons into Higgs particles*, *Phys. Rev. Lett.* **39** (1977) 1304.

[83] K.G. Chetyrkin, B.A. Kniehl and M. Steinhauser, *Decoupling relations to $O(\alpha_S^3)$ and their connection to low-energy theorems*, *Nucl. Phys. B* **510** (1998) 61 [hep-ph/9708255] [INSPIRE].

[84] Y. Schröder and M. Steinhauser, *Four-loop decoupling relations for the strong coupling*, *JHEP* **01** (2006) 051 [hep-ph/0512058] [INSPIRE].

JHEP09(2020)143

[85] K. Chetyrkin, J. Kühn and C. Sturm, *QCD decoupling at four loops*, *Nucl. Phys. B* **744** (2006) 121.

[86] M. Krämer, E. Laenen and M. Spira, *Soft gluon radiation in Higgs boson production at the LHC*, *Nucl. Phys. B* **511** (1998) 523 [hep-ph/9611272] [INSPIRE].

[87] B.A. Kniehl, A.V. Kotikov, A.I. Onishchenko and O.L. Veretin, *Strong-coupling constant with flavor thresholds at five loops in the anti-MS scheme*, *Phys. Rev. Lett.* **97** (2006) 042001 [hep-ph/0607202] [INSPIRE].

[88] F. Dulat and B. Mistlberger, *Real-virtual-virtual contributions to the inclusive Higgs cross section at N3LO*, arXiv:1411.3586 [INSPIRE].

[89] F. Dulat, S. Lionetti, B. Mistlberger, A. Pelloni and C. Specchia, *Higgs-differential cross section at NNLO in dimensional regularisation*, *JHEP* **07** (2017) 017 [arXiv:1704.08220] [INSPIRE].

[90] F. Dulat, B. Mistlberger and A. Pelloni, *Differential Higgs production at N^3LO beyond threshold*, *JHEP* **01** (2018) 145 [arXiv:1710.03016] [INSPIRE].

[91] C. Anastasiou, C. Duhr, F. Dulat, F. Herzog and B. Mistlberger, *Real-virtual contributions to the inclusive Higgs cross-section at N^3LO*, *JHEP* **12** (2013) 088 [arXiv:1311.1425] [INSPIRE].

[92] C. Duhr, T. Gehrmann and M. Jaquier, *Two-loop splitting amplitudes and the single-real contribution to inclusive Higgs production at N^3LO*, *JHEP* **02** (2015) 077 [arXiv:1411.3587] [INSPIRE].

[93] C. Duhr and T. Gehrmann, *The two-loop soft current in dimensional regularization*, *Phys. Lett. B* **727** (2013) 452 [arXiv:1309.4393] [INSPIRE].

[94] P. Nogueira, *Automatic Feynman graph generation*, *J. Comput. Phys.* **105** (1993) 279.

[95] C. Anastasiou, C. Duhr, F. Dulat and B. Mistlberger, *Soft triple-real radiation for Higgs production at N3LO*, *JHEP* **07** (2013) 003 [arXiv:1302.4379] [INSPIRE].

[96] C. Anastasiou et al., *Higgs boson gluon-fusion production beyond threshold in N^3LO QCD*, *JHEP* **03** (2015) 091 [arXiv:1411.3584] [INSPIRE].

[97] C. Anastasiou, C. Duhr, F. Dulat, E. Furlan, F. Herzog and B. Mistlberger, *Soft expansion of double-real-virtual corrections to Higgs production at N^3LO*, *JHEP* **08** (2015) 051 [arXiv:1505.04110] [INSPIRE].

[98] M.A. Ebert, B. Mistlberger and G. Vita, *Transverse momentum dependent PDFs at N^3LO*, arXiv:2006.05329 [INSPIRE].

[99] M.A. Ebert, B. Mistlberger and G. Vita, *Calculation of differential collinear expansions at N^3LO*, in preparation.

[100] E. Remiddi and J.A.M. Vermaseren, *Harmonic polylogarithms*, *Int. J. Mod. Phys. A* **15** (2000) 725 [hep-ph/9905237] [INSPIRE].

[101] A.B. Goncharov, *Multiple polylogarithms and mixed Tate motives*, math/0103059 [INSPIRE].

[102] C. Duhr, H. Gangl and J.R. Rhodes, *From polygons and symbols to polylogarithmic functions*, *JHEP* **10** (2012) 075 [arXiv:1110.0458] [INSPIRE].

[103] C. Duhr, *Hopf algebras, coproducts and symbols: an application to Higgs boson amplitudes*, *JHEP* **08** (2012) 043 [arXiv:1203.0454] [INSPIRE].

JHEP09(2020)143

[104] C. Duhr and F. Dulat, *PolyLogTools — Polylogs for the masses*, *JHEP* **08** (2019) 135 [arXiv:1904.07279] [INSPIRE].

[105] E. Panzer, *Algorithms for the symbolic integration of hyperlogarithms with applications to Feynman integrals*, *Comput. Phys. Commun.* **188** (2015) 148 [arXiv:1403.3385] [INSPIRE].

[106] M.A. Ebert and F.J. Tackmann, *Resummation of transverse momentum distributions in distribution space*, *JHEP* **02** (2017) 110 [arXiv:1611.08610] [INSPIRE].

[107] L.A. Harland-Lang, A.D. Martin, P. Motylinski and R.S. Thorne, *Parton distributions in the LHC era: MMHT 2014 PDFs*, *Eur. Phys. J. C* **75** (2015) 204 [arXiv:1412.3989] [INSPIRE].

[108] M.A. Ebert et al., *SCETlib: a C++ package for numerical calculations in QCD and soft-collinear effective theory*, DESY-17-099 (2018).

[109] D. Kang, C. Lee and I.W. Stewart, *Using* 1*-jettiness to measure* 2 *jets in DIS* 3 *ways*, *Phys. Rev. D* **88** (2013) 054004 [arXiv:1303.6952] [INSPIRE].

[110] D. Kang, C. Lee and I.W. Stewart, *Analytic calculation of* 1*-jettiness in DIS at* $O(\alpha_s)$, *JHEP* **11** (2014) 132 [arXiv:1407.6706] [INSPIRE].

[111] M.-x. Luo, T.-Z. Yang, H.X. Zhu and Y.J. Zhu, *Quark transverse parton distribution at the next-to-next-to-next-to-leading order*, *Phys. Rev. Lett.* **124** (2020) 092001 [arXiv:1912.05778] [INSPIRE].

[112] D.W. Kolodrubetz, I. Moult and I.W. Stewart, *Building blocks for subleading helicity operators*, *JHEP* **05** (2016) 139 [arXiv:1601.02607] [INSPIRE].

[113] I. Feige, D.W. Kolodrubetz, I. Moult and I.W. Stewart, *A complete basis of helicity operators for subleading factorization*, *JHEP* **11** (2017) 142 [arXiv:1703.03411] [INSPIRE].

[114] I. Moult, I.W. Stewart and G. Vita, *A subleading operator basis and matching for* $gg \to H$, *JHEP* **07** (2017) 067 [arXiv:1703.03408] [INSPIRE].

[115] C.-H. Chang, I.W. Stewart and G. Vita, *A subleading power operator basis for the scalar quark current*, *JHEP* **04** (2018) 041 [arXiv:1712.04343] [INSPIRE].

[116] M. Beneke, M. Garny, R. Szafron and J. Wang, *Anomalous dimension of subleading-power* N*-jet operators*, *JHEP* **03** (2018) 001 [arXiv:1712.04416] [INSPIRE].

[117] M. Beneke, M. Garny, R. Szafron and J. Wang, *Anomalous dimension of subleading-power* N*-jet operators. Part II*, *JHEP* **11** (2018) 112 [arXiv:1808.04742] [INSPIRE].

[118] I. Moult, I.W. Stewart, G. Vita and H.X. Zhu, *First subleading power resummation for event shapes*, *JHEP* **08** (2018) 013 [arXiv:1804.04665] [INSPIRE].

[119] I. Moult, I.W. Stewart and G. Vita, *Subleading power factorization with radiative functions*, *JHEP* **11** (2019) 153 [arXiv:1905.07411] [INSPIRE].

[120] I. Moult, I.W. Stewart, G. Vita and H.X. Zhu, *The soft quark Sudakov*, *JHEP* **05** (2020) 089 [arXiv:1910.14038] [INSPIRE].

[121] A. Bhattacharya, I. Moult, I.W. Stewart and G. Vita, *Helicity methods for high multiplicity subleading soft and collinear limits*, *JHEP* **05** (2019) 192 [arXiv:1812.06950] [INSPIRE].

[122] T. Becher and M. Neubert, *Infrared singularities of scattering amplitudes in perturbative QCD*, *Phys. Rev. Lett.* **102** (2009) 162001 [*Erratum ibid.* **111** (2013) 199905] [arXiv:0901.0722] [INSPIRE].

JHEP09(2020)143

[123] G.P. Korchemsky and A.V. Radyushkin, *Renormalization of the Wilson loops beyond the leading order*, *Nucl. Phys. B* **283** (1987) 342 [INSPIRE].

[124] S. Moch, J.A.M. Vermaseren and A. Vogt, *The three loop splitting functions in QCD: the nonsinglet case*, *Nucl. Phys. B* **688** (2004) 101 [hep-ph/0403192] [INSPIRE].

[125] A. Vogt, S. Moch and J.A.M. Vermaseren, *The three-loop splitting functions in QCD: the singlet case*, *Nucl. Phys. B* **691** (2004) 129 [hep-ph/0404111] [INSPIRE].

[126] O.V. Tarasov, A.A. Vladimirov and A. Zharkov, *The Gell-Mann-Low function of QCD in the three loop approximation*, *Phys. Lett. B* **93** (1980) 429 [INSPIRE].

[127] S.A. Larin and J.A.M. Vermaseren, *The three loop QCD β-function and anomalous dimensions*, *Phys. Lett. B* **303** (1993) 334 [hep-ph/9302208] [INSPIRE].

JHEP09(2020)143